

# Nanosize rutile titania particle synthesis *via* a hydrothermal method without mineralizers

S. T. Aruna, S. Tirosh and A. Zaban\*

Department of Chemistry, Bar-Ilan University, Ramat-Gan, 52900, Israel.  
 E-mail: zabana@mail.biu.ac.il

Received 2nd March 2000, Accepted 28th June 2000  
 First published as an Advance Article on the web 31st August 2000

A new approach for direct synthesis of well-shaped pure rutile titania nanocrystals by hydrothermal synthesis is reported. The synthesis of the 20 nm rutile particles from titanium isopropoxide and pH 0.5 nitric acid is achieved by vigorous stirring of the solution during the hydrothermal treatment. The significant effect of the stirring and long aging control experiments suggest that, at this composition, most of the condensation to TiO<sub>2</sub> occurs during the autoclaving step. The large colloid size distribution and the formation of the anatase structure in the absence of stirring are attributed to the inhomogeneity developed in the solution under the extreme conditions of the hydrothermal process. The significance of the new method is the elimination of the commonly used mineralizers that can induce impurities into the nanocrystals, in addition to the improved colloid shape in comparison with standard procedures.

## Introduction

In recent years, there has been increasing interest in the application of nanosize titania for catalysts and supports, ceramics, inorganic membranes, gas sensing, water purification and solar energy conversion.<sup>1–7</sup> Nanosize titania is attractive for these applications because of its large effective surface area which enhances the surface reactions. Titania exists in three main crystallographic forms that exist at standard pressure; anatase, rutile and brookite. Each structure exhibits different physical properties, such as refractive index, chemical reactivity and photochemical reactivity.<sup>8</sup> Each application that is based on titania requires a specific crystal structure and, usually, also a specific size.<sup>7,9–13</sup> Thus, it is important to develop synthetic methods in which the size and structure of the nanocrystals can be controlled.

Anatase titania has been prepared by various methods, such as sol–gel,<sup>5,14</sup> hydrothermal,<sup>12,15</sup> combustion synthesis<sup>16</sup> and inert-gas condensation.<sup>17–20</sup> There are many reports on the synthesis of anatase particles with sizes ranging from 5 nm to several microns and a variety of shapes, for various applications. Similar methods have been used for the synthesis of rutile titania. However, unlike anatase, it was found that the synthesis of small well-shaped rutile particles is much more difficult. Such colloids, prepared under acidic conditions using mainly TiCl<sub>4</sub>, result in large or irregularly shaped particles.<sup>21</sup> The only way to obtain small rutile TiO<sub>2</sub> nanoparticles reported so far involves the use of TiCl<sub>4</sub> and mineralizers, like SnCl<sub>4</sub>, NH<sub>4</sub>Cl, NaCl or SnO<sub>2</sub>.<sup>4,13</sup>

Usually, the mineralizers are selected in such a way that the TiO<sub>2</sub> will crystallize in the rutile structure. SnO<sub>2</sub> is the most widely used mineralizer, acting as a semicoherent surface for the transforming rutile to grow on.<sup>4,13,22</sup> The particles obtained using mineralizers by the hydrothermal method were rod-like or broom-like aggregates with sizes of 100 by 10 nm.<sup>15,20,23</sup> Other attempts to prepare small rutile titania particles using ammonium chloride as a mineralizer resulted in agglomerated hairy spheroid particles.<sup>15</sup> Sol–gel methods, where again mineralizers were used to stabilize the rutile structure, also did not provide fine nanoparticulate powders.<sup>13</sup> Moreover, the mineralizer-based synthesis described above suffers from the presence of contaminant salts and, hence, the solutions have to be repeatedly washed to eliminate the salts. To the best of our

knowledge, the preparation of spherical nanosize rutile titania has not yet been reported. In addition, regardless of shape, pure rutile nanosize titania has not been prepared from titanium alkoxide without a mineralizer.

We report here on the preparation of pure rutile titania particles having a diameter of 20 nm *via* highly controlled hydrothermal synthesis. The direct synthesis to rutile TiO<sub>2</sub> is based on titanium isopropoxide and pH 0.5 nitric acid. It does not involve the use of mineralizers that can induce impurities into the nanocrystals. The direct synthesis of the pure rutile nanoparticles is achieved by the addition of vigorous stirring during the autoclaving step of the synthesis. In the absence of stirring, under the same conditions, a mixture of anatase and rutile was formed. Long aging experiments and the synthesis results suggest that a major part of the condensation takes place in the more acidic regions during the hydrothermal treatment. Thus, stirring that maintains homogeneity in the solution during the hydrothermal process is highly important when a homogeneous product is required.

## Experimental

The synthesis of rutile titania involved the following steps. An aliquot of 5 mL of titanium isopropoxide and 5 mL of dry isopropanol were added dropwise to a well-stirred 40 mL solution of pH 0.5 nitric acid. The solution was stirred for 8 h, whereupon the isopropanol was evaporated by heating the solution to 82 °C. The resulting solution was transferred into a Teflon container and placed in a titanium autoclave (Parr instrument). As mentioned above, the key factor in the preparation of pure rutile titania is the stirring during the autoclaving process. The solution was stirred throughout the autoclaving period using a homemade magnet-based system. The autoclaving process was carried out at 250 °C for 26 h with a heating rate of 15 °C min<sup>-1</sup>. Each synthesis was carried out twice, with and without stirring, the latter serving as a reference.

The long aging experiments during the titania synthesis involved the following steps. As in the preparation of the small rutile particles, 5 mL of titanium isopropoxide and 5 mL of dry isopropanol were added dropwise to 40 mL of well-stirred nitric acid. The pH of the solutions was 0.5 in one case and 2.0

in the other. The solutions were then aged at room temperature for 6 months.

X-ray diffraction patterns were used to determine the identity, quantity and size of each crystal phase present. The powder XRD patterns were recorded using a Rigaku 2028 X-ray diffractometer with Cu-K $\alpha$  radiation. The average crystallite size ( $D$ ) of the powders was calculated from the Scherrer formula.<sup>24</sup> The quantitative ratio between the anatase and rutile phases was calculated from the ratios of areas under background-subtracted {100} anatase and {110} rutile peaks using the method outlined by Spurr and Myers.<sup>25</sup> TEM imaging was carried out with a JEOL-JEM 100SX transmission electron microscope. Samples for TEM analysis were prepared by dispersing TiO<sub>2</sub> onto TEM copper grids thinly coated with amorphous carbon. Surface area measurements of the powders were carried out with a standard BET surface area analyzer (Micromeritics Gemini III 2375).

## Results and discussion

Two sets of titania colloids were prepared by hydrothermal synthesis of titanium isopropoxide and pH 0.5 nitric acid using a similar procedure. During the hydrothermal treatment one set was vigorously stirred while the other, as is usually the case, was not stirred. Fig. 1 shows the powder XRD patterns of the two sets prepared with and without stirring. From the XRD patterns, it is clear that, in the case of the stirred sample (Fig. 1a), pure rutile titania is obtained. The unstirred sample (Fig. 1b) is a mixture consisting of 61% rutile, with the rest being in the anatase form. The percentage of rutile was calculated using the ratios of areas under the {101} anatase and the {110} rutile peaks.<sup>5,25</sup> The particle size calculated from the X-ray line broadening by the Scherrer formula is  $20.4 \pm 2$  nm for the stirred sample (pure rutile), with the corresponding sizes of the unstirred sample crystallites being  $54.0 \pm 5$  nm for the rutile crystallites and  $21.6 \pm 2$  nm for the anatase. Fig. 2 shows transmission electron micrographs of the two sets of titania colloids. From the TEM pictures it is evident that, in case of the stirred sample, the particles are small and well shaped, *i.e.* almost spherical (Fig. 2a), whereas the TEM picture of the unstirred sample shows bigger particles of irregular shape (Fig. 2b). Fig. 3 shows size distribution histograms of the stirred and unstirred colloidal powders counting 250 particles of each sample. The average size of the stirred rutile titania is 17.5 nm, with a standard deviation of 6.9 (Fig. 3a). The average size of the mixed anatase and rutile colloids made without stirring is 28.6 nm, with a larger standard deviation of 11.9 (Fig. 3b). The TEM pictures show that stirring during the hydrothermal process not only drives the formation of pure rutile, but also improves the particle size distribution.

The mechanism for direct anatase or rutile titania formation may be explained using the concepts of the partial charge

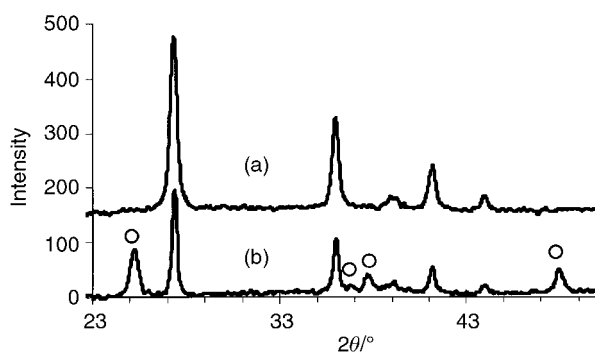


**Fig. 1** Powder XRD patterns of titania obtained by hydrothermal synthesis: (a) with stirring, showing pure rutile titania, and (b) without stirring, showing a mixture of anatase and rutile (the circles denote peak positions corresponding to anatase titania).

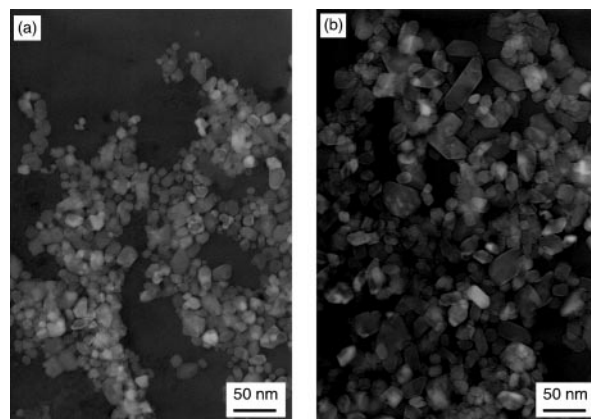


**Fig. 2** Transmission electron micrographs of titania prepared by hydrothermal synthesis: (a) with stirring and (b) without stirring. The particles prepared with stirring are smaller and more uniform.

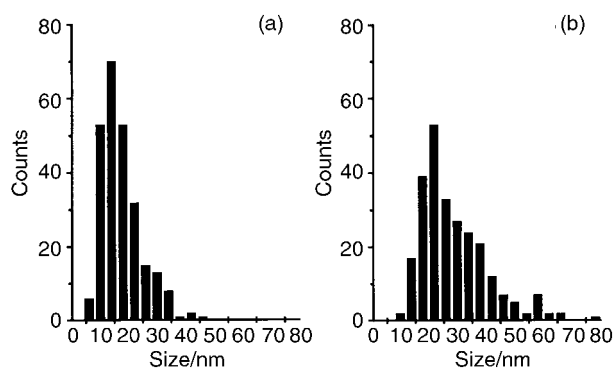


**Fig. 3** Size distribution histograms measured from the TEM pictures presented in Fig. 2: (a) titania prepared with stirring and (b) without stirring. The particles prepared with stirring are smaller and their size distribution is narrower.

model.<sup>26</sup> According to this model, hydrolysis of the titanium cation occurs at low pH. The first hydrolysis step leads to the formation of  $[\text{Ti}(\text{OH})(\text{OH}_2)_5]^{3+}$  species which are stable under strong acid conditions. These species are not able to condense because of the positive charge of the hydroxo group.<sup>26</sup> When acidity is not sufficiently low to stabilize these precursors, deprotonation takes place, forming  $[\text{Ti}(\text{OH})_2(\text{OH}_2)_4]^{2+}$ , which also does not condense, probably because of spontaneous intramolecular oxolation to  $[\text{TiO}(\text{OH}_2)_5]^{2+}$ .<sup>27,28</sup> Condensation to both rutile and anatase starts when the solution activity is high enough to allow further deprotonation to  $[\text{TiO}(\text{O}-\text{H})(\text{OH}_2)_4]^+$ , which can undergo intramolecular deoxolation to  $[\text{Ti}(\text{OH})_3(\text{OH}_2)_3]^+$ , depending on the exact pH.<sup>26</sup> In the lower pH region, deoxolation does not occur and oxolation leads to linear growth along the equatorial plane of the cations. This reaction, followed by oxolation between the resulting linear chains, leads to rutile formation. At higher pH values, when deoxolation takes place, condensation can proceed along apical directions, leading to the skewed chains of the anatase structure. In other words, the structure of the precursor cation, which is affected by the exact pH, determines the resulting crystal structure.<sup>20,21,26,29</sup>

The acidity maintained during the preparation of the pure rutile, pH 0.5, is probably in the range that prevents condensation, as is evident from the following long aging experiments. Titanium isopropoxide was hydrolyzed in pH 0.5 nitric acid, using the same procedure as for the preparation of the pure rutile, and the solution was aged for 6 months. The XRD pattern and TEM image of the hydrolysis products are presented in Fig. 4a and 5a, respectively. The XRD measurement shows that no crystallization has occurred, even after

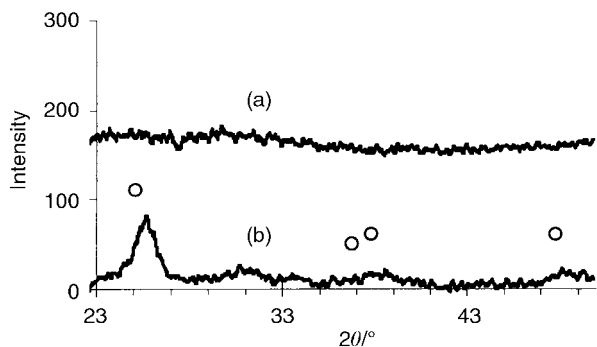


**Fig. 4** Powder XRD patterns of the hydrolysis products of titanium isopropoxide in nitric acid: (a) at pH 0.5, showing no crystallization, and (b) at pH 2 showing weakly crystalline anatase titania (the circles denote peaks corresponding to anatase titania).

extended aging of the solution. The TEM image shows that colloids were not formed during the aging period. In a reference experiment that was carried out in a similar manner, except using pH 2 nitric acid, different results were obtained. Fig. 4b and 5b present the XRD pattern and the TEM image of the pH 2 products. In contrast to the hydrolysis at pH 0.5, the XRD and TEM measurements show that weakly crystalline anatase  $\text{TiO}_2$  colloids were formed during the process. These results cannot be regarded as evidence for the absence of any condensation at pH 0.5. However, they show that at pH 0.5 most of the condensation and crystallization observed after the hydrothermal treatment is probably the result of the hydrothermal process.

During the hydrothermal treatment, the solution is exposed to high temperature ( $250^\circ\text{C}$ ) and pressure (560 psi). The results showing that the  $\text{TiO}_2$  crystals are formed during this process suggest that the condensation is made possible by these conditions. Various thermodynamic and kinetic effects are expected to influence the temperature/pressure-induced condensation.<sup>30</sup> One such effect, for example, is the significant increase of the pH at temperatures higher than  $150^\circ\text{C}$ ,<sup>31,32</sup> which should allow condensation towards the rutile structure, followed by condensation to the anatase structure at even higher pH values.<sup>26</sup> Regardless of the exact mechanism by which the hydrothermal treatment induces the condensation, it is expected that the homogeneity of the solution during the treatment will affect the homogeneity of the products. This may include parameters such as size, shape and even crystal structure, if, for example, pH gradients are developed in the solution.<sup>33</sup>

During the autoclaving step of the hydrothermal synthesis, local gradients of temperature and concentration are unavoidable. The outside heating causes the former, while the latter is caused by evaporation of some of the solution components. Both the concentration and temperature gradients can drive pH inhomogeneity. Under such conditions, one can expect that colloids of various properties will be formed, depending on the local conditions each particle experiences. In other words, the results presented above showing that stirring during the hydrothermal process drives the formation of pure rutile, and improves the particle size distribution in comparison with the unstirred sample, can be explained by the homogeneity achieved in the stirred synthesis.

The surface area of the rutile titania colloids prepared by this method is  $45\text{ m}^2\text{ g}^{-1}$ , as measured by BET. The high surface area is important for applications such as rutile-based dye-sensitized solar cells,<sup>23</sup> solar reflecting shields,<sup>9,10</sup> gas sensing<sup>4</sup> and catalysis.<sup>4,13</sup> Some of these applications involve operation at high temperatures in which sintering of the nanoparticles causes a decrease of the surface area. It was reported that the major cause for the surface area reduction is the enhanced sintering during the transformation from anatase to rutile.<sup>4</sup>

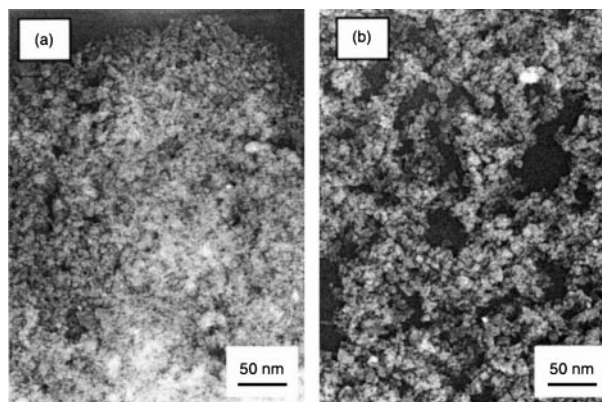


**Fig. 5** Transmission electron micrographs of the hydrolysis products of titanium isopropoxide in nitric acid: (a) at pH 0.5, showing no colloids, and (b) at pH 2 showing small colloids.

Rutile titania containing 19 mol%  $\text{SnO}_2$  mineralizer was found to experience less sintering, but the role of the  $\text{SnO}_2$  in the stabilization was not clear.<sup>4</sup> The stability of the pure rutile synthesized in this work at high temperatures was tested using the diameter of the nanocrystals as a probe. Fig. 6 presents the crystallite size of rutile nanoparticles that were exposed to various temperatures between  $400$  and  $800^\circ\text{C}$  for 3 h. The crystallite size was calculated from the X-ray line broadening. Fig. 6 shows that, up to  $700^\circ\text{C}$ , the crystallite diameter did not change significantly, indicating that the rutile particles experience a relatively low sintering rate in comparison with the sintering rate at  $800^\circ\text{C}$ . This seems to indicate that the presence of  $\text{SnO}_2$  does not affect the sintering process. Therefore, the rutile titania prepared in the present work should be suitable for high temperature applications, including catalytic membranes.

## Conclusions

Pure rutile titania particles having a diameter of 20 nm were synthesized *via* a highly controlled hydrothermal process. Long aging experiments show that, in the more acidic regions, condensation does not occur at ambient conditions, in agreement with the well-established metallic ion partial charge model. The synthesis results show that condensation takes place mostly during the hydrothermal treatment, where inhomogeneity of the solution can develop due to the extreme conditions of the process. Thus, stirring of the solution during the hydrothermal process is necessary when a homogenous product is required. The rutile titania nanocrystals prepared by this method have a large surface area and are relatively stable at high temperatures.

The small rutile colloids prepared in this work are superior to similar materials made using mineralizers. The new colloids are almost spherical, unlike the irregular shapes (usually needle-like) obtained previously. The new colloids are the smallest

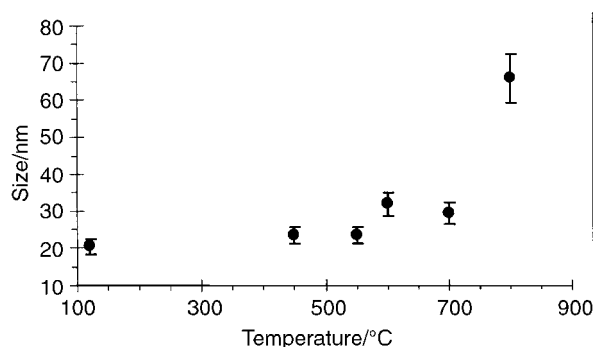


**Fig. 6** Crystallite size of rutile titania exposed to various temperatures for 3 h.

reported so far, exhibiting a narrow size distribution. Finally, their preparation does not involve the use of mineralizers, which contaminate the samples and induce undesirable characteristics.

## Acknowledgements

This research was supported by the Israel Science Foundation funded by the Israel Academy of Sciences and Humanities.

## References

- 1 D. F. Ollis, E. Pelizzetti and N. Serpone, *Environ. Sci. Technol.*, 1996, **5**, 1523.
- 2 D. H. Solomon and D. G. Hawthorne, *Chemistry of Paints and Fillers*, Wiley, New York, 1983, ch. 2.
- 3 K.-N. P. Kumar, K. Keizer and A. J. Burggraaf, *J. Mater. Chem.*, 1993, **3**, 1141.
- 4 K.-N. P. Kumar, K. Keizer and A. J. Burggraaf, *J. Mater. Sci. Lett.*, 1994, **13**, 59.
- 5 A. Gribb and J. Banfield, *Am. Mineral.*, 1997, **82**, 717.
- 6 P. V. Kamat, in *Native and Surface Modified Semiconductor Nanoclusters*, ed. K. D. Karlin, John Wiley and Sons Inc., New York, 1997, pp. 273–343.
- 7 T. Gerfin, M. Gratzel and L. Walder, in *Molecular and Supermolecular Surface Modification of Nanocrystalline TiO<sub>2</sub> Films: Charge Separating and Charge Injecting Devices*, ed. K. D. Karlin, John Wiley and Sons Inc., New York, 1997, pp. 345–353.
- 8 A. F. Wells, *Structural Inorganic Chemistry*, Clarendon Press, Oxford, 1975.
- 9 T. M. J. Nilsson and G. A. Niklasson, *Sol. Energy Mater. Sol. Cells*, 1995, **37**, 93.
- 10 C. Granqvist and T. Eviksson, in *Materials for Radiative Cooling to Low Temperatures*, ed. C. Granqvist, Pergamon Press, Oxford, 1991, p. 168.
- 11 P. Kamat, *Chem. Rev.*, 1993, **93**, 267.
- 12 C.-C. Wang and J. Y. Ying, *Chem. Mater.*, 1999, **11**, 3113.
- 13 K.-N. P. Kumar, K. Keizer, A. J. Burggraaf, T. Okubo and H. Nagamoto, *J. Mater. Chem.*, 1993, **3**, 923.
- 14 M. Schneider and A. Baiker, *J. Mater. Chem.*, 1992, **2**, 587.
- 15 H. Cheng, J. Ma, Z. Zhao and L. Qi, *Chem. Mater.*, 1995, **7**, 663.
- 16 S. T. Aruna and K. C. Patil, *J. Mater. Synth. Process.*, 1996, **4**, 175.
- 17 R. W. Siegel and J. A. Eastman, *Mater. Res. Soc. Symp. Proc.*, 1989, **132**, 3.
- 18 J. Rubio, J. L. Oteo, M. Villegas and P. Duran, *J. Mater. Sci.*, 1997, **32**, 643.
- 19 P. Murugavel, M. Kalaiselvam, A. R. Raju and C. N. R. Rao, *J. Mater. Chem.*, 1997, **7**, 1433.
- 20 S. Kratochvil and E. Matijevic, *Adv. Ceram. Mater.*, 1987, **2**, 798.
- 21 F. Cavani, E. Foresti, F. Parrinello and F. Trifiro, *Appl. Catal.*, 1998, **38**, 311.
- 22 P. K. Nair, F. Mizukami, J. Nair, M. Salou, Y. Oosawa, H. Izutsu, K. Maeda and T. Okubo, *Mater. Res. Bull.*, 1998, **33**, 1495.
- 23 N. G. Park, G. Schlichthorl, J. van de Lagemaat, H. M. Cheong, A. Mascarenhas and A. J. Frank, *J. Phys. Chem.*, 1999, **103**, 3308.
- 24 B. D. Cullity, *Elements of X-Ray Diffraction*, Addison-Wesley Publishing Company, Inc., London, 1978.
- 25 R. A. Spurr and H. Myers, *Anal. Chem.*, 1957, **29**, 760.
- 26 M. Henry, J. P. Jolivet and J. Livage, in *Aqueous Chemistry of Metal Cations, Hydrolysis, Condensation, and Complexation*, ed. R. Reisfeld and C. K. Jorgensen, Springer-Verlag, Berlin, 1992, p. 155.
- 27 J. D. Ellis, A. K. Thompson and A. G. Sykes, *Inorg. Chem.*, 1976, **15**, 3172.
- 28 J. D. Ellis and A. G. Sykes, *J. Chem. Soc., Dalton Trans.*, 1973, 537.
- 29 C. J. Barbe, F. Arendse, P. Comte, M. Jirousek, F. Lenzmann, V. Shklover and M. Gratzel, *J. Am. Ceram. Soc.*, 1997, **80**, 3157.
- 30 P. W. Atkins, *Physical Chemistry*, Oxford University Press, Oxford, 1986.
- 31 E. L. Shock, *Am. J. Sci.*, 1995, **295**, 496.
- 32 B. N. Ryzhenko, S. D. Malinin and A. V. Plyasunov, *Petrology*, 1997, **5**, 45.
- 33 A. Zaban, S. T. Aruna, S. Tirosh, B. A. Gregg and Y. Mastai, *J. Phys. Chem. B*, 2000, **104**, 4130.